Exchange Functionals and Basis Set Comparisons for Theoretical Studies of ZnO nonoclusters

Duwage C. Perera[a] **and Jayendran C. Rasaiah**[a,1]

[a]Department of Chemistry, University of Maine, Orono, ME 04469

This manuscript was compiled on May 13, 2021

Catalysts made of nano-scaled metal oxide clusters can push the limits of chemical reactions in the manufacture of paints, cosmetics, and pharmaceuticals. The ZnO clusters can also act as semiconductors with a wide band gap of 3.4 eV at 300 K, and are prospective photocatalysts in many reactions including H_2 production in water splitting reactions. In this project, we studied the structural (geometry) and electronic properties (vertical detachment energy and electron affinity) of ZnO monomers and dimers that form model ZnO clusters, using density functional theory (DFT) with many different exchange functionals and 29 basis sets to optimize their choice. We compared the singlet-triplet energy gaps of small ZnO clusters to find the optimal ZnO cluster size and the best theoretical method to investigate their photocatalytic water splitting activity.

Our results show that B3LYP/DGDZVP2 level of exchange functional/basis set theory is the most efficient and fastest of the ones considered. Comparison of the singlet-triplet energy gaps shows that the trimer $(ZnO)_3$, with an energy gap of 58.66 k cal/mol, is approximately equal to the energy of a visible photon at 555 nm and a HOMO-LUMO gap of 4.4 eV, and is the best choice amongst the $(ZnO)_n$ clusters of different sizes when the number of monomers n in the clusters ranges from 1 to 6. We used the Gaussian16 software package for all the calculations.

Zinc Oxide Clusters | Density Functional Theory | Basis Set Comparison |Exchange functional | Vertical Detachment Energy | Electron Affinity

Metal oxides have been used in many ways over the past decades. Depending on the metal, the oxides can be utilized as catalysts, sensors, in food industry, cosmetics, medicine and solar cells. Scaling down from macro to nano, both the physical and chemical properties of each metal oxide are changed, and nano scaled metal oxide clusters can become promising material to push the limits of their applications (1–5). Accordingly, there has been a growing interest in studying the properties of metal oxide nanoclusters using both theoretical and experimental methods (6–9). Zinc oxide (ZnO) is such a material with potential applications of interest in many industries including paint, cosmetics, pharmaceuticals and catalysis (10–19). ZnO nanoparticles also have been identified as potential adsorbents of organic dyes, gasses and heavy metals (20, 21). It is a semiconductor with a wide band gap of 3.4 eV at 300K and has unique magnetic, optical and electronic properties (22–24). Moreover those properties can change considerably when the particle dimension and size change to the nanoscale. ZnO nanoparticles with different morphologies including nanorods, nanosheets, nanowires and nanoflowers can be synthesized using thermal decomposition, the sol-gel method, forced hydrolysis and hydro-thermal method (25, 26).

The structural and electronic properties of ZnO clusters have been studied both experimentally and theoretically. Bovhyra et al. used density functional theory (DFT) to study the structural and electronic properties of $(ZnO)_n$ (n= 34, 60) nanoclusters (27). From their results, the most stable $(ZnO)_{34}$ nanoclusters were fullerene - like hollow structures and the most energetically favorable $(ZnO)_{60}$ had a sodalite - type structure made with seven $(ZnO)_{12}$ clusters with common quadrangle edges. The energy range of the highest occupied molecular orbital (HOMO) and the lowest unoccupied molecular orbital (LUMO) for those clusters are 1.93 - 2.40 eV. A study by Woodley et al. reported the stable and low energy meta-stable structures of $(ZnO)_n$, (n=1-32) clusters using evolutionary algorithm techniques (28). Their findings include, 2D rings for n=2-7 that are less than 0.8 nm in diameter and spheroid bubbles upto n=32 that are less than 1.2 nm in diameter.

Another theoretical study by Szakacs et.al shows the relative thermodynamic stability of two different ZnO nanocluster shapes; needles and plates. The electronic structure calculations of ZnO needles and plates nanoclusters shows,the Zn_iO_i; where i= 6, 9, 12, 15 and 18, needles have higher stability that increased with the number of stacked rings. They also studied Zn_3O_3 as the most successful building block to form larger clusters rather than adding individual or pairs of Zn and O atoms (29).

An extensive theoretical study on the structural and electronic properties of $(ZnO)_n$, $n \leq 168$ has been carried out by Chen et al (30). Their major findings include the presence of new magic numbers for $(ZnO)_n$ for structures at n= 78, 100, 132 and 168 with the particle stability increasing for structures with single to double and triple layered octahedral cage morphologies. The higher stability in multilayered particles is due to the lack of terminal surface atoms and the effective interlayer stacking of hexagonal cells. Chen et al. have also summarized the stability of small ZnO clusters. The lowest energy isomers for $(ZnO)_n$ n=3-5 are predicted to be ringlike 2- dimensional (2D) structures that have higher stability compared to the open and 3D structures .

To fill the gap in information lacking in previous investigations of anionic ZnO clusters, Castlemen Jr et al. investigated the relative stabilities and electronic properties of small ZnO clusters using density functional theory (DFT) with both B3LYP and PBEPBE functionala and 6-311++G(3d), aug-cc-pvQZ and LanL2DZ basis sets (31), and have compared their calculations with published experimental results. This combined experimental and theoretical study reported the

The authors declare no competing financial interest

[1]To whom correspondence should be addressed. E-mail: rasaiah@maine.edu

mass spectrum of anionic Zn_nO_m (n=1-6 and m=1-7) clusters and predicted the ground state geometries and stabilities of Zn_3O_m and $Zn_3O_m^-$ (m=3-5).

In this paper, we set the stage for further investigations of the photocatalytic properties of ZnO clusters by examining the structural and electronic properties of the monomer and dimer of ZnO using different functionals and basis sets to investigate improved methods of property analysis. Moreover, we calculate the energy gap of singlet and triplet states of small ZnO clusters and HOMO-LUMO energy gaps with selected basis sets as a first step towards understanding the photocatalytic properties of ZnO clusters, and specifically as a first step towards the study of H_2 and O_2 production by water splitting reaction. To the best of our knowledge, this has not been previously reported theoretically for ZnO clusters.

Computational Method

We first chose the monomer and the dimer of ZnO to study their structural and electronic properties using different functionals in DFT. We chose 30 different basis sets by using standard and augmented Dunning and Pople style bases: 3-21G, 6-31G, 6-31+G, 6-31++G, 6-311G, 6-311++G, 6-31G(d), 6-31G(d,p), 6-31+G(d), 6-31+G(2d), 6-31+G(2d,p), 6-31+G(2df,p), 6-31+G(2df,2p), 6-31+G(3df,2p), 6-31++G(d), 6-31++G(d,p), 6-311+G(d), 6-311G(d,p), 6-311++G(d), 6-311++G(d,p), cc-PVQZ, aug-cc-PVDZ, aug-cc-PVTZ, DGDZVP, DGDZVP2, Def2TZVP, LANL2DZ, CEP-121G, TZVP, QZVP.

First we optimized the ZnO monomer and dimer structures using B3LYP, B3PW91, PBEPBE, BVP86, BP86, M06 exchange functionals in DFT and the CCSD(T) method with 30 different basis sets. We analyzed bond lengths, bond angles and mulliken charges on atoms as structural properties and the vertical detachment energy (VDE) and electron affinity (EA) as electronic properties of each optimized structure. Additionally we compared the HOMO-LUMO gap, the difference between singlet and triplet energies and infrared spectra of (ZnO)n clusters, with n=1-6, to evaluate candidates with suitable photocatalytic properties. We compared our calculated values with previously published experimental results (31) to identify the best basis set candidates.

All geometry optimization and structural and electronic property calculations were carried out using the Gaussian 16 software package (32) and GaussView 6 graphical interface (33).

Results and Discussion

A. Comparison of Structural Properties. Geometry optimization is the process of finding the positions of nuclei for which the potential energy is minimized. We optimized the ZnO monomer and dimer and compared the structural properties using the different DFT and CCSD(T) method with 30 different basis sets. Figure 1 illustrates the optimized monomer (a) and dimer (b) structures of ZnO using DFT with B3LYP/DGDZVP2 combination of exchange functional and basis set. We selected the bond lengths (2Zn - 1O for both monomer and dimer as shown in the Figure 1), and dimer bond angles (2Zn-1O-3Zn and 1O-2Zn-4O) and mulliken charges on each atom (labeled as in the Figure 1) as characteristic structural properties.

(a) ZnO Monomer **(b)** ZnO Dimer

Fig. 1. Optimized (a) monomer and (b) dimer structures at B3LYP/ DGDZVP2 level of theory. Zn and O atoms are represented by light blue and red colors respectively.

Table 1. Monomer Bond Length (Zn-O)/Å

	Functional	DFT						CCSD(T)
	Basis Set	B3LYP	B3PW91	PBEPBE	BVP86	BP86	M06	
1	3-21G	1.609	1.607	1.603	1.603	1.603	1.602	1.658
2	6-31G	1.695	1.687	1.684	1.683	1.683	1.685	1.748
3	6-31+G	1.740	1.727	1.731	1.729	1.730	1.730	1.780
4	6-31++G	1.740	1.727	1.731	1.729	1.730	1.730	1.780
5	6-311G	1.818	1.799	1.791	1.791	1.792	1.822	1.829
6	6-311++G	1.740	1.728	1.731	1.730	1.730	1.730	1.768
7	6-31G(d)	1.670	1.663	1.661	1.660	1.661	1.658	1.700
8	6-31G(d,p)	1.670	1.663	1.661	1.660	1.661	1.658	1.700
9	6-31+G(d)	1.712	1.700	1.705	1.704	1.705	1.699	1.730
10	6-31+G(2d)	1.712	1.700	1.705	1.704	1.705	1.700	1.729
11	6-31+G(2d,p)	1.712	1.700	1.705	1.704	1.705	1.700	1.729
12	6-31+G(2df,p)	1.710	1.698	1.703	1.702	1.703	1.698	1.718
13	6-31+G(2df,2p)	1.710	1.698	1.703	1.702	1.703	1.698	1.718
14	6-31+G(3df,2p)	1.708	1.696	1.701	1.700	1.701	1.695	1.715
15	6-31++G(d)	1.712	1.700	1.705	1.704	1.705	1.699	1.730
16	6-31++G(d,p)	1.712	1.700	1.705	1.704	1.705	1.699	1.730
17	6-311+G(d)	1.720	1.709	1.713	1.712	1.713	1.709	1.731
18	6-311G(d,p)	1.791	1.773	1.766	1.766	1.767	1.793	1.788
19	6-311++G(d)	1.720	1.709	1.713	1.712	1.713	1.709	1.731
20	6-311++G(d,p)	1.720	1.709	1.713	1.712	1.713	1.709	1.731
21	cc-PVQZ	1.707	1.696	1.700	1.699	1.700	1.694	1.712
22	aug-cc-PVDZ	1.712	1.701	1.705	1.704	1.705	1.699	1.714
23	aug-cc-PVTZ	1.710	1.699	1.703	1.702	1.703	1.696	1.719
24	DGDZVP	1.726	1.713	1.715	1.715	1.716	1.714	1.755
25	DGDZVP2	1.718	1.706	1.708	1.707	1.707	1.706	1.746
26	Def2TZVP	1.713	1.701	1.705	1.705	1.705	1.702	1.717
27	LANL2DZ	1.764	1.754	1.765	1.764	1.765	1.753	1.783
28	CEP-121G	1.732	1.719	1.720	1.719	1.720	1.718	1.757
29	TZVP	1.722	1.709	1.711	1.710	1.711	1.711	1.740
30	QZVP	1.709	1.697	1.702	1.701	1.702	1.696	1.714

Table 2. Dimer Bond Length (Zn-O)/Å

	Functional	DFT						CCSD(T)
	Basis Set	B3LYP	B3PW91	PBEPBE	BVP86	BP86	M06	
1	3-21G	1.825	1.822	1.832	1.831	1.832	1.813	1.858
2	6-31G	1.891	1.882	1.901	1.900	1.900	1.874	1.925
3	6-31+G	1.921	1.908	1.936	1.934	1.935	1.901	1.946
4	6-31++G	1.921	1.908	1.936	1.934	1.935	1.901	1.946
5	6-311G	1.925	1.909	1.942	1.940	1.941	1.900	-
6	6-311++G	1.915	1.904	1.931	1.928	1.929	1.896	1.932
7	6-31G(d)	1.856	1.847	1.863	1.862	1.863	1.841	1.868
8	6-31G(d,p)	1.856	1.847	1.863	1.862	1.863	1.841	1.868
9	6-31+G(d)	1.890	1.879	1.902	1.901	1.902	1.873	1.898
10	6-31+G(2d)	1.887	1.876	1.900	1.899	1.899	1.870	1.894
11	6-31+G(2d,p)	1.887	1.876	1.900	1.899	1.899	1.870	1.894
12	6-31+G(2df,p)	1.886	1.875	1.899	1.898	1.899	1.869	1.884
13	6-31+G(2df,2p)	1.886	1.875	1.899	1.898	1.899	1.869	1.884
14	6-31+G(3df,2p)	1.884	1.872	1.896	1.895	1.896	1.867	-
15	6-31++G(d)	1.890	1.879	1.902	1.901	1.902	1.873	1.898
16	6-31++G(d,p)	1.890	1.879	1.902	1.901	1.902	1.873	1.898
17	6-311+G(d)	1.898	1.888	1.913	1.911	1.912	1.881	1.897
18	6-311G(d,p)	1.899	1.884	1.915	1.913	1.914	1.876	-
19	6-311++G(d)	1.898	1.888	1.913	1.911	1.912	1.881	1.897
20	6-311++G(d,p)	1.898	1.888	1.913	1.911	1.912	1.881	1.897
21	aug-cc-PVDZ	1.888	1.879	1.901	1.899	1.900	1.870	1.892
22	aug-cc-PVTZ	1.886	1.876	1.899	1.897	1.897	1.867	-
23	DGDZVP	1.907	1.896	1.922	1.921	1.922	1.886	1.922
24	DGDZVP2	1.900	1.890	1.913	1.911	1.912	1.882	1.917
25	Def2TZVP	1.891	1.881	1.905	1.904	1.904	1.873	1.884
26	LANL2DZ	1.932	1.923	1.953	1.951	1.952	1.916	1.948
27	CEP-121G	1.908	1.897	1.921	1.920	1.921	1.892	1.922
28	TZVP	1.898	1.888	1.913	1.911	1.912	1.881	1.902
29	QZVP	1.885	1.875	1.897	1.896	1.897	1.867	1.876

The monomer and dimer bond lengths calculated using 30

different basis sets and 6 different DFT functionals and CCSD(T) method are shown in the Tables 1 and 2 respectively. All other results are tabulated in the supporting information (SI) document.

We compared the bond lengths of both monomer and dimer with the published experimental values (the bond length of Zn-O is 1.719 Å and 1.787 for its anion. The bond lengths, calculated using B3LYP functional vary widely from 1.609Å-1.818Å. However, basis sets 6-311+G(d), 6-311++G(d),6-311++G(d,p) and DGDZVP2 show bond lemgths in good agreement with the experimental value within ±0.01 difference. Monomer bond lengths calculated using the B3LYP functional are comparably closer to experiment to within the first decimal using the CCSD(T) method. The Zn-O bond length in the dimer is longer than in the monomer.

Dimer bond angles, 2Zn-1O-3Zn and 1O-2Zn-4O are shown in Figure 1(b) and presented in Table 3. The 2Zn-1O-3Zn angle is between 73.17° - 79.59°, while the 1O-2Zn-4O angles, which are larger, are between 100.06°-106.86°. In comparison, a theoretical study by Ugalde et.al on the stability of global minimum for small ZnO clusters shows the 1O-2Zn-4O angle is 103.7° and the Zn-O bond length is 1.892 Å for the ZnO dimer using B3LYP functional and the relativistic compact effective core potentials and shared-exponent basis set of Stevens, Krauss, Basch and Jasien (SKBJ), in good agreement with our results. (34)

B. Comparison of Electronic Properties. Amongst the electronic properties, we compare the expermental (35, 36) electron affinities (EA) and vertical detachment energies (VDE) of both ZnO monomer and dimer with our calculated values using equation 1 and 2 (37).

Electron Affinity(EA)=E(optimized neutral molecule)-E(optimized anion)[1]

Vertical Detachment Energy(VDE)=E(neutral at optimized anion geometry) –E(optimized anion)[2]

The difference in energy between the neutral molecule and the negative ion of the molecule in their ground state is the EA of a molecule. Positive EA values indicate thermodynamically stable negative ions. All the EA values for the monomer recorded in the Table 4 are positive except for the CCSD(T)/6-311G(d,p) and CCSD(T)/aug-cc-PVDZ caculations. The positive EA values for the monomer are in the range of 0.567 - 2.538 eV. According to an experimental study by Fancher et.al and Kim et.al using photoelectron spectra of ZnO and ZnO^-, the EA of the monomer ZnO is 2.088 ±0.010 eV (35, 36). From Table 4, 6-31+G, 6-31++G,6-31+G(3df,2p) and aug-cc-PVTZ basis sets from CCSD(T) method we see that they agree with the experimental value. Comparing the DFT results, from B3LYP functional DGDZVP2 and CEP-121G; B3PW91 functional LANL2DZ; PBEPBE functional cc-PVQZ and aug-cc-PVDZ; and M06 functional cc-PVQC basis sets are also in accord with the experimental value.

Table 3. Dimer Bond Angle (2Zn-1O-3Zn)/° in black and Dimer Bond Angle (1O-2Zn-4O)/° in orange

	Functional	DFT						CCSD(T)
	Basis Set	B3LYP	B3PW91	PBEPBE	BVP86	BP86	M06	
1	3-21G	74.17	74.31	73.27	73.17	73.14	74.62	75.05
		105.83	105.69	106.73	106.83	106.86	105.38	104.96
2	6-31G	74.87	74.75	73.26	73.22	73.20	74.91	75.06
		105.13	105.25	106.74	106.78	106.80	105.09	104.94
3	6-31+G	76.89	76.49	75.59	75.65	75.63	76.79	75.97
		103.11	103.51	104.41	104.35	104.37	103.21	104.05
4	6-31++G	76.89	76.49	75.59	75.65	75.63	76.79	75.97
		103.11	103.51	104.41	104.35	104.37	103.21	104.05
5	6-311G	77.13	77.25	76.09	76.06	76.05	77.04	-
		102.87	102.75	103.91	103.94	103.95	102.96	-
6	6-311++G	77.20	76.85	75.83	75.90	75.88	76.99	76.67
		102.80	103.15	104.17	104.10	104.12	103.01	103.37
7	6-31G(d)	74.94	74.81	73.50	73.49	73.47	74.97	74.97
		105.06	105.19	106.50	106.51	106.53	105.03	105.03
8	6-31G(d,p)	74.94	74.81	73.50	73.49	73.47	74.97	74.97
		105.06	105.19	106.50	106.51	106.53	105.03	105.03
9	6-31+G(d)	77.17	76.80	75.92	75.98	75.94	76.91	76.40
		102.83	103.20	104.08	104.02	104.06	103.09	103.60
10	6-31+G(2d)	77.13	76.70	75.83	75.90	75.89	76.92	76.27
		102.87	103.30	104.17	104.10	104.11	103.08	103.72
11	6-31+G(2d,p)	77.13	76.70	75.83	75.90	75.89	76.92	76.27
		102.87	103.30	104.17	104.10	104.11	103.08	103.72
12	6-31+G(2df,p)	77.11	76.68	75.80	75.87	75.86	76.90	76.36
		102.89	103.32	104.20	104.13	104.14	103.10	103.64
13	6-31+G(2df,2p)	77.11	76.68	75.80	75.87	75.86	76.90	76.35
		102.89	103.32	104.20	104.13	104.14	103.10	103.65
14	6-31+G(3df,2p)	76.86	76.47	75.57	75.63	75.61	76.62	-
		103.14	103.53	104.43	104.37	104.39	103.38	-
15	6-31++G(d)	77.17	76.80	75.92	75.98	75.94	76.91	76.40
		102.83	103.20	104.08	104.02	104.06	103.09	103.60
16	6-31++G(d,p)	77.17	76.80	75.92	75.98	75.94	76.91	76.40
		102.83	103.20	104.08	104.02	104.06	103.09	103.60
17	6-311+G(d)	77.40	77.09	76.11	76.16	76.14	77.11	76.97
		102.60	102.91	103.89	103.84	103.86	102.89	103.03
18	6-311G(d,p)	76.82	77.00	75.87	75.85	75.83	76.78	-
		103.18	103.00	104.13	104.15	104.17	103.22	-
19	6-311++G(d)	77.40	77.09	76.11	76.16	76.14	77.11	76.97
		102.60	102.91	103.89	103.84	103.86	102.89	103.03
20	6-311++G(d,p)	77.40	77.09	76.11	76.16	76.14	77.11	76.97
		102.60	102.91	103.89	103.84	103.86	102.89	103.03
21	aug-cc-PVDZ	77.28	76.90	76.00	76.05	76.04	76.90	76.51
		102.72	103.10	104.00	103.95	103.96	103.10	103.49
22	aug-cc-PVTZ	77.31	76.93	76.04	76.08	76.08	76.84	-
		102.68	103.07	103.96	103.92	103.92	103.16	-
23	DGDZVP	77.04	76.81	76.07	76.12	76.10	76.83	76.60
		102.96	103.19	103.93	103.88	103.90	103.17	103.39
24	DGDZVP2	77.29	77.04	76.32	76.36	76.34	76.96	76.71
		102.70	102.96	103.68	103.64	103.66	103.04	103.28
25	Def2TZVP	77.18	76.83	75.97	76.01	76.00	76.75	77.08
		102.82	103.17	104.03	103.99	104.00	103.25	102.91
26	LANL2DZ	79.94	79.59	78.96	78.99	78.97	79.35	78.57
		100.06	100.41	101.04	101.01	101.03	100.65	101.43
27	CEP-121G	76.45	76.13	75.24	75.30	75.29	76.03	75.60
		103.55	103.87	104.76	104.70	104.71	103.97	104.39
28	TZVP	76.44	76.18	75.11	75.20	75.19	76.17	76.36
		103.56	103.82	104.89	104.80	104.81	103.83	103.64
29	QZVP	77.35	76.97	76.08	76.13	76.12	76.82	76.97
		102.65	103.03	103.92	103.87	103.88	103.18	103.03

The EA values of the ZnO dimer reported in Table 5 are positive. and are in the range of 0.27 - 2.43 eV and comparatively lower than the monomer values.

The minimum energy needed to eject an electron, without changing the internuclear distances from the negative ion of a molecule in its ground state is defined as the vertical displacemnt energy VDE. The literature value of VDE for the ZnO monomer is 2.03 eV (35, 36).

Table 6 and 7 show the calculated values of VDE for both ZnO monomer and dimer. For the monomer the values are between 0.27 - 7.29 eV. Most of them are close to 2.00 eV including the B3LYP/DGDZVP2 level of theory (which is 2.16 eV).

Table 4. Monomer EA/eV

	Functional	DFT						CCSD(T)
	Basis Set	B3LYP	B3PW91	PBEPBE	BVP86	BP86	M06	
1	6-31G	1.89	1.944	1.539	1.944	1.701	1.89	1.215
2	6-31+G	2.295	2.403	2.322	2.457	2.484	2.538	2.025
3	6-31++G	2.295	2.403	2.322	2.457	2.484	2.538	2.025
4	6-311G	1.188	1.107	0.81	0.567	0.594	1.296	-
5	6-311++G	2.403	2.322	2.16	2.511	2.241	2.268	1.863
6	6-31G(d)	1.728	1.782	1.647	1.782	1.809	1.728	1.269
7	6-31G(d,p)	1.728	1.782	1.647	1.782	1.809	1.728	1.269
8	6-31+G(d)	2.268	2.376	2.295	2.457	2.187	2.268	1.863
9	6-31+G(2d)	2.16	2.268	2.187	2.349	2.349	2.187	1.89
10	6-31+G(2d,p)	2.16	2.268	2.187	2.349	2.349	2.187	1.89
11	6-31+G(2df,p)	2.43	2.241	2.16	2.295	2.322	2.43	1.836
12	6-31+G(2df,2p)	2.43	2.241	2.16	2.295	2.322	2.43	1.836
13	6-31+G(3df,2p)	2.403	2.214	2.133	2.295	2.322	2.403	2.079
14	6-31++G(d)	2.268	2.376	2.295	2.457	2.187	2.268	1.863
15	6-31++G(d,p)	2.268	2.376	2.295	2.457	2.187	2.268	1.863
16	6-311+G(d)	2.268	2.16	2.268	2.349	2.376	2.403	1.863
17	6-311G(d,p)	1.053	0.945	0.648	0.945	0.702	1.431	-0.081
18	6-311++G(d)	2.268	-	2.268	2.349	2.376	2.403	1.863
19	6-311++G(d,p)	2.268	2.16	2.268	2.349	2.376	2.403	1.863
20	cc-PVQZ	2.268	2.187	2.079	2.16	2.187	2.052	1.809
21	aug-cc-PVDZ	2.268	2.133	2.079	2.214	2.214	2.349	-1.431
22	aug-cc-PVTZ	2.16	2.349	2.268	2.376	2.376	2.214	2.025
23	DGDZVP	1.917	1.836	1.62	1.701	1.701	1.809	1.296
24	DGDZVP2	2.025	1.971	1.728	1.782	1.809	1.917	1.323
25	Def2TZVP	2.079	2.241	1.917	2.295	2.295	2.133	1.674
26	LANL2DZ	1.836	2.025	1.728	2.025	1.782	-	1.404
27	CEP-121G	2.025	2.079	1.917	2.052	2.241	2.133	1.485
28	TZVP	1.89	1.755	1.485	1.836	1.593	1.89	1.107
29	QZVP	2.322	2.214	2.106	2.214	2.241	2.268	1.809

Table 5. Dimer Electron Affinity /eV

	Functional	DFT						CCSD(T)
	Basis Set	B3LYP	B3PW91	PBEPBE	BVP86	BP86	M06	
1	3-21G	1.67	1.62	1.62	1.89	1.62	1.35	1.08
2	6-31G	1.73	1.62	1.62	1.89	1.89	1.62	1.35
3	6-31+G	2.16	2.16	2.16	2.43	2.43	2.16	1.62
4	6-31++G	2.16	2.16	2.16	2.43	2.43	2.16	1.62
5	6-311G	0.54	0.54	0.54	0.54	0.81	0.54	-
6	6-311++G	2.16	1.89	2.16	2.43	2.16	-	-
7	6-31G(d)	1.62	1.62	1.62	1.62	1.62	1.62	-
8	6-31G(d,p)	1.62	1.62	1.62	1.62	1.62	1.62	-
9	6-31+G(d)	2.16	2.16	1.89	2.43	2.16	2.16	1.62
10	6-31+G(2d)	2.16	1.89	1.89	2.43	2.16	2.16	1.89
11	6-31+G(2d,p)	2.16	1.89	1.89	2.43	2.16	2.16	1.89
12	6-31+G(2df,p)	2.16	2.16	1.89	2.16	2.16	2.16	1.89
13	6-31+G(2df,2p)	2.16	2.16	1.89	2.16	2.16	2.16	1.89
14	6-31+G(3df,2p)	1.89	1.89	2.16	2.16	2.16	2.16	-
15	6-31++G(d)	2.16	2.16	1.89	2.43	2.16	2.16	1.62
16	6-31++G(d,p)	2.16	2.16	1.89	2.43	2.16	2.16	1.62
17	6-311+G(d)	2.16	1.89	2.16	2.16	2.16	2.16	1.89
18	6-311G(d,p)	0.54	0.54	0.27	0.54	0.54	0.27	-
19	6-311++G(d)	2.16	1.89	2.16	2.16	2.16	2.16	1.89
20	6-311++G(d,p)	2.16	1.89	2.16	2.16	2.16	2.16	1.89
21	aug-cc-PVDZ	1.89	1.89	1.89	2.16	2.43	1.89	-
22	aug-cc-PVTZ	2.16	1.89	2.16	2.16	2.16	1.89	-
23	DGDZVP	1.62	1.62	1.62	1.89	1.89	1.35	1.35
24	DGDZVP2	1.62	1.62	1.62	1.89	1.89	1.89	-
25	Def2TZVP	1.89	2.16	1.89	1.89	1.89	1.89	-
26	LANL2DZ	1.89	1.89	1.62	1.89	1.89	1.89	1.62
27	CEP-121G	2.16	1.89	2.16	2.16	1.89	1.89	1.62
28	TZVP	1.62	1.35	1.62	1.62	1.62	1.62	-
29	QZVP	1.89	1.89	2.16	2.16	2.16	1.89	-

Table 6. Monomer VDE/eV

	Functional	DFT						CCSD(T)
	Basis Set	B3LYP	B3PW91	PBEPBE	BVP86	BP86	M06	
1	6-31G	1.89	1.89	1.62	1.89	1.89	1.89	1.35
2	6-31+G	2.43	2.43	2.43	2.43	2.43	2.7	2.16
3	6-31++G	2.43	2.43	2.43	2.43	2.43	2.7	2.16
4	6-311G	1.35	1.35	7.29	0.54	0.54	1.35	0.27
5	6-311++G	2.43	2.43	2.16	2.43	2.43	2.43	1.89
6	6-31G(d)	1.89	1.89	1.62	1.89	1.89	1.89	1.35
7	6-31G(d,p)	1.89	1.89	1.62	1.89	1.89	1.89	1.35
8	6-31+G(d)	2.43	2.43	2.43	2.43	2.16	2.43	1.89
9	6-31+G(2d)	2.16	2.43	2.16	2.43	2.43	2.16	1.89
10	6-31+G(2d,p)	2.16	2.43	2.16	2.43	2.43	2.16	1.89
11	6-31+G(2df,p)	2.43	2.16	2.16	2.43	2.43	2.43	1.89
12	6-31+G(2df,2p)	2.43	2.16	2.16	2.43	2.43	2.43	1.89
13	6-31+G(3df,2p)	2.43	2.16	2.16	2.43	2.43	2.43	2.16
14	6-31++G(d)	2.43	2.43	2.43	2.43	2.16	2.43	1.89
15	6-31++G(d,p)	2.43	2.43	2.43	2.43	2.16	2.43	1.89
16	6-311+G(d)	2.43	2.16	2.43	2.43	2.43	2.43	1.89
17	6-311G(d,p)	1.35	1.08	7.29	7.29	7.29	1.62	-
18	6-311++G(d)	2.43	-	2.43	2.43	2.43	2.43	1.89
19	6-311++G(d,p)	2.43	2.16	2.43	2.43	2.43	2.43	1.89
20	cc-PVQZ	2.43	2.16	2.16	2.16	2.16	2.16	1.89
21	aug-cc-PVDZ	2.43	2.16	2.16	2.16	2.16	2.43	1.89
22	aug-cc-PVTZ	2.16	2.43	2.43	2.43	2.43	2.43	2.16
23	DGDZVP	1.89	1.89	1.62	1.89	1.89	1.89	1.35
24	DGDZVP2	2.16	2.16	1.90	1.89	1.89	2.16	1.35
25	Def2TZVP	2.16	2.16	1.89	2.43	2.43	2.16	1.62
26	LANL2DZ	1.89	2.16	1.89	2.16	1.89	-	1.35
27	CEP-121G	4.05	2.16	1.89	2.16	2.16	2.16	1.62
28	TZVP	1.89	1.89	1.62	1.89	1.62	2.16	1.08
29	QZVP	2.43	2.16	2.16	2.16	2.16	2.43	1.89

The VDE values of the following functionals and basis sets: the B3LYP functional, and 6-31+G(2d), 6-31+G(2d,p), aug-cc-PVTZ and Def2TZVP basis sets ; the B3PW91 functional, and 6-31+G(2df,p), 6-31+G(2df,2p), 6-31+G(3df,2p), 6-311+G(d), 6-311++G(d,p), cc-PVQZ, aug-cc-PVDZ, DGDZVP2,Def2TZVP,LANL2DZ,CEP-121G and QZVP basis sets ; the PBEPBE functional, and 6-311++G, 6-31+G(2d), 6-31+G(2d,p), 6-31+G(2df,p), 6-31+G(2df,2p), 6-31+G(3df,2p), cc-PVQZ, aug-cc-PVDZ and QZVP; BVP86 functional, and cc-PVQZ, aug-cc-PVDZ,LANL2DZ, CEP-121G and QZVP, BP86 functional, 6-31+G(2d), 6-31+G(2d,p), cc-PVQZ, DGDZVP2, Def2TZVP, CEP-121G and TZVP bais sets ; the M06 functional, and 6-31+G(2d), 6-31+G(2d,p), cc-PVQZ, DGDZVP2, Def2TZVP, CEP-121G and TZVP baisi sets ; the CCSD(T) method, with the 6-31+G, 6-31++G, 6-31+G(3df,2p) and aug-cc-PVTZ basis sets are 2.16 eV with is close to the experimental value recorded within ± 0.13 eV. The VDE values for dimer are in the range of 0.27 -2.43 eV. In the table 7, only CCDS(T)/6-311G(d,p) shows a negative VDE value.

Considering both the geometrical and electronic properties, we suggest that the combination of the B3LYP exchange functional and DB3LYPGDZVP2 basis set (B3LYP/DB3LYPGDZVP2) would be the most cost effective and reliable method to use in the study of ZnO clusters as catalysts for which the EA and VDE closely agree with the experimental values.

Table 7. Dimer VDE/eV

	Functional	DFT						CCSD(T)
	Basis Set	B3LYP	B3PW91	PBEPBE	BVP86	BP86	M06	
1	3-21G	1.62	1.62	1.62	1.89	1.62	1.35	-
2	6-31G	1.89	1.62	1.62	1.89	1.89	1.62	1.35
3	6-31+G	2.16	2.16	2.43	2.43	2.43	2.16	1.89
4	6-31++G	2.16	2.16	2.43	2.43	2.43	2.16	1.89
5	6-311G	0.54	0.54	0.54	0.54	0.81	0.54	-
6	6-311++G	2.16	2.16	2.16	2.43	2.16	-	-
7	6-31G(d)	1.62	1.62	1.62	1.62	1.62	1.62	-
8	6-31G(d,p)	1.62	1.62	1.62	1.62	1.62	1.62	-
9	6-31+G(d)	2.16	2.16	1.89	2.43	2.16	2.16	1.62
10	6-31+G(2d)	2.16	1.89	1.89	2.43	2.16	2.16	1.89
11	6-31+G(2d,p)	2.16	1.89	1.89	2.43	2.16	2.16	1.89
12	6-31+G(2df,p)	2.16	2.16	1.89	2.43	2.16	2.16	-
13	6-31+G(2df,2p)	2.16	2.16	1.89	2.43	2.16	2.16	-
14	6-31+G(3df,2p)	2.16	1.89	2.16	2.16	2.16	2.16	-
15	6-31++G(d)	2.16	2.16	1.89	2.43	2.16	2.16	1.62
16	6-31++G(d,p)	2.16	2.16	1.89	2.43	2.16	2.16	1.62
17	6-311+G(d)	2.16	1.89	2.16	2.16	2.16	2.16	1.89
18	6-311G(d,p)	0.54	0.54	0.27	0.54	0.54	0.27	-0.27
19	6-311++G(d)	2.16	1.89	2.16	2.16	2.16	2.16	1.89
20	6-311++G(d,p)	2.16	1.89	2.16	2.16	2.16	2.16	1.89
21	aug-cc-PVDZ	1.89	2.16	1.89	2.43	2.43	2.16	-
22	aug-cc-PVTZ	2.16	1.89	2.16	2.16	2.16	2.16	-
23	DGDZVP	1.62	1.62	1.62	1.89	1.89	1.35	1.35
24	DGDZVP2	1.62	1.62	1.62	1.89	1.89	1.89	-
25	Def2TZVP	1.89	2.16	1.89	1.89	2.16	2.16	-
26	LANL2DZ	1.89	1.89	1.62	1.89	1.89	1.89	1.62
27	CEP-121G	2.16	1.89	2.16	2.16	2.16	2.16	1.62

Table 8. HOMO-LUMO gap in eV

Cluster Size	Basis set			
	6-311++G	DGDZVP	DGDZVP2	aug-cc-PVDZ
1	2.29	2.33	2.35	2.36
2	2.52	2.58	2.63	2.69
3	4.17	4.36	4.42	4.35
4	4.39	4.59	4.66	4.56
5	4.56	4.72	4.79	4.69
6	3.52	3.71	3.76	3.68

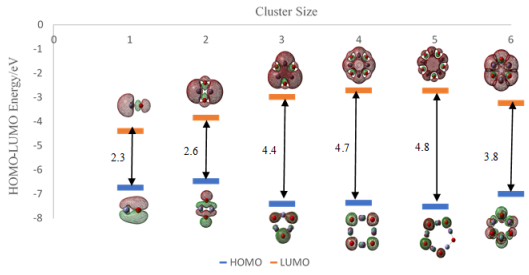

Fig. 2. HOMO-LUMO gap of (ZnO)n, n=1-6 using B3LYP/DGDZVP2. Images use the coarse grid method and isoval=0.02.

After choosing suitable basis sets for our study of the properties of ZnO, we also investigated suitable cluster sizes to study photocatalysis. Our primary goal was to identify a reliable photocatalyst from amongst ZnO clusters to produce H_2 and O_2 by splitting two water molecules.

The energy gap between HOMO and LUMO is one of the important parameters that identify cluster stability. We compare the HOMO-LUMO gap of small ZnO clusters, where the cluster size is from 1-6 in Table 8 using the B3LYP functional and 6-311++G, DGDZVP, DGDZVP2 and aug-cc-PVDZ basis sets. Results using B3LYP/DGDZVP2 level of theory are shown in the Figure 2 and other results are shown in the SI document.

Cluster sizes 4 and 5 have relatively higher HOMO-LUMO gaps (4.66 eV and 4.79 eV respectively using B3LYP/DGDZVP2 method) indicating that they would be relatively less efficient than the other neutral clusters. The $(ZnO)_3$ and $(ZnO)_6$ have lower HOMO-LUMO energy gaps(4.42 eV and 3.76 eV using the same method) compared to the 4^{th} and 5^{th} clusters, and indicate that the 3^{th} and 6^{th} ZnO clusters have comparably higher reactivity. When considering the photocatalytic water splitting reaction to produce H_2, the minimum photon energy required for the overall reaction is 1.23 eV which indicates that all the small ZnO nanoclusters studied are possible candidates to catalyze the photosplitting of water.

We have also calculated the vibrational frequencies in order to check the stability of the optimized geometries. Infrared spectra for $(ZnO)_n$; n=1-6 are shown in Figure 3 and all the relevant frequency values for the monomer, dimer and their anions are tabulated in the SI document. There were no imaginary vibrational frequencies in our study of any of the clusters. The monomer ZnO has one wide peak at 708 cm^{-1}. The dimer ZnO has three major peaks at 213 cm^{-1}, 441 cm^{-1} and 566 cm^{-1} frequencies. The $(ZnO)_3$ has a major peak at 648 cm^{-1} and a minor peak at 221 cm^{-1}, $(ZnO)_4$ has a major peak at 735 cm^{-1} and two minor peaks at 176 cm^{-1} and 225 cm^{-1}, $(ZnO)_5$ has one major peak at 801 cm^{-1} and 3 minor peaks at 174 cm^{-1}, 221 cm^{-1} and 518 cm^{-1} and the $(ZnO)_6$ two major peaks at 385 cm^{-1} and 581 cm^{-1} and a minor peak at 491 cm^{-1} frequencies.

The optimized energies of the singlet and the first excited triplet state of $(ZnO)_n$, n=1-6 are calculated using the selected methods. The details are shown in the SI document. The energy difference of the singlet and the first excited triplet state are displayed in the table 9.

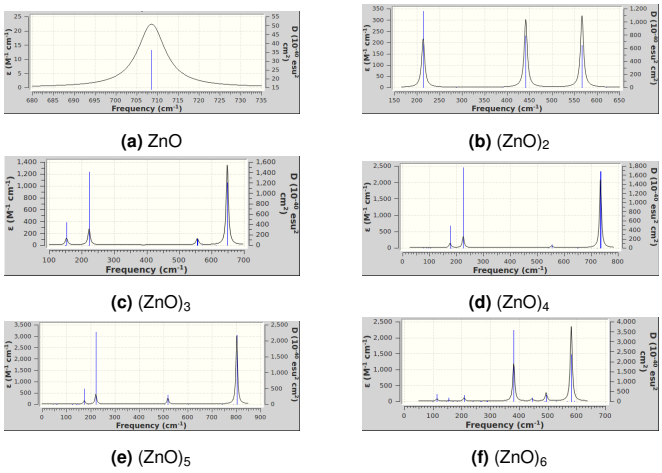

Fig. 3. Calculated infrared spectra for $(ZnO)_n$ structures (a)n=1, (b)n=2, (c)n=3, (d)n=4, (e)n=5 and (f)n=6.

H_2 production in the water splitting reaction is an endothermic reaction that requires two H_2O molecules. The heat of formation of H_2O is -57.8 ±0.02 kCal/mol at 298 K temperature, which is approximately comparable to the energy of two photons at 500 nm (38).

Table 9. Singlet-Triplet energy difference in k cal/mol at B3LYP functional

	Basis set	Cluster Size (n)					
		1	2	3	4	5	6
1	3-21G	9.78	7.17	55.34	71.95	76.64	58.15
2	6-31+G	-3.73	13.14	52.82	63.63	68.71	54.67
3	6-31++G	-3.73	13.14	52.82	63.63	68.71	54.80
4	6-311G	-14.36	6.01	53.50	54.75	62.44	53.13
5	6-311++G	-3.87	13.65	53.02	63.90	69.05	54.98
6	6-31G(d)	2.12	17.70	59.70	69.41	77.65	61.57
7	6-31+G(d)	36.29	17.02	34.36	69.09	74.56	59.23
8	6-31+G(2d)	36.35	18.34	58.44	69.59	74.70	58.96
9	6-31+G(2d,p)	36.35	18.34	58.44	69.59	74.70	58.96
10	6-31+G(2df,p)	36.09	18.08	58.27	69.46	74.59	58.88
11	6-31+G(2df,2p)	36.09	18.08	58.27	69.46	74.59	58.88
12	6-31+G(3df,2p)	36.11	18.68	58.95	69.83	75.18	59.61
13	6-31++G(d)	36.29	17.02	57.55	69.09	74.56	59.23
14	6-31++G(d,p)	36.29	17.02	57.55	69.09	74.56	59.23
15	Aug-ccPVDZ	35.21	18.55	58.52	69.73	74.84	58.90
16	Aug-ccPVTZ	34.90	18.26	58.26	69.67	74.87	58.98
17	DGDZVP	34.49	14.74	57.33	69.45	74.77	58.77
18	DGDZVP2	34.85	16.05	58.66	73.22	76.39	59.93
19	Def2TZVP	34.30	16.48	57.65	69.17	74.48	58.32
20	TZVP	33.48	15.29	56.12	67.04	72.00	57.47

The role of a photocatalyst is to absorb the energy of visible light and elevate the ground state electrons of a molecule to an excited state that enables the reaction to occur faster through a lowering of the activation barrier. Studying the excited state of the desired reaction is thus important. But excited open shell singlet states are difficult or nearly impossible to investigate using current density functional theory methods. Since the energy difference between the excited singlet state and the triplet state is comparably low, we consider the triplet state as the approximate excited singlet state energy.

When comparing our calculated results of the energy difference between the singlet and triplet state of small ZnO clusters, n=1 and 2 have values lower than than 57.8 kCal/mol while n=4 and 5 have higher values. Cluster size 3 and 6 have relatively values closer to the energy of 2 visible photons which would be desired cluster systems to study the photocatalytic water splitting reaction to produce H_2 and O_2 using 2 water molecules in the presence of ZnO nanolcusters as the catalyst.

Conclusion

We have investigated the structural and electronic properties of ZnO monomer and dimer and vibrational frequencies of both structures to choose suitable basis sets and exchange functionals to study photocatalytic effects of ZnO nanoclusters on water splitting. We also studied the singlet-triplet energy difference and HOMO-LUMO gap of $(ZnO)_n$; n=1-6 to select the best cluster size of ZnO as a photocatalyst. By comparing our calculated values with experimental values, we find that the B3LYP/DGDZVP2 combination of exchange functional and basis set would be reliable and optimal in calculating the properties of ZnO nanoclusters using DFT with a relatively low computational time compared to other methods (e.g. CCSD(T)). From the singlet -triplet energy comparisons, both n=3 and n=6 nanocluster systems are also possible photocatalysts to use in the formation of H_2 and O_2 in a water splitting reaction, and we suggest that the $(ZnO)_3$ rather than the $(ZnO)_6$ is the better of the two photocatalysts considering the complexity of the reaction.

Author Affiliations

ORCID

Duwage Charitha Perera 0000-0003-4237-138X
Jayendran C. Rasaiah 0000-0002-4453-7438

Corresponding Author

Email: rasaiah@maine.edu

Notes

The authors declare no competing financial interest.

Acknowledgment

We thank Stephen Cousins, Bruce Segee and staff of the University of Maine High Performance Computing Group for their technical assistance and allotment of computer time.We also thank Eric Lovejoy for his assistance.

Supporting Information Appendix (SI)

The Supporting Information (SI) document is available for free of charge.

References

1. SA Claridge, et al., Cluster-Assembled Materials. *ACS Nano* **3**, 244–255 (2009) Publisher: American Chemical Society.
2. P Jena, AW Castleman, Clusters: A bridge across the disciplines of physics and chemistry. *Proc. Natl. Acad. Sci.* **103**, 10560–10569 (2006) Publisher: National Academy of Sciences Section: Introductory Perspective.
3. HG Byun, I Kim, HS Kwon, GT Bae, Comparisons of the Functional and Basis Set Combinations for Silicon Oxide Clusters: A Density Functional Theory Study: Comparisons of the Functional and Basis Set Combinations. *Bull. Korean Chem. Soc.* **38**, 1310–1315 (2017).
4. S Li, DA Dixon, Benchmark Calculations on the Electron Detachment Energies of MO3- and M2O6- (M = Cr, Mo, W). *The J. Phys. Chem. A* **111**, 11908–11921 (2007) Publisher: American Chemical Society.

5. GT Bae, B Dellinger, RW Hall, Density Functional Calculation of the Structure and Electronic Properties of CunOn (n = 18) Clusters. *The J. Phys. Chem. A* **115**, 2087–2095 (2011) Publisher: American Chemical Society.
6. L Guo, YL Ji, H Xu, P Simon, Z Wu, Regularly Shaped, Single-Crystalline ZnO Nanorods with Wurtzite Structure. *J. Am. Chem. Soc.* **124**, 14864–14865 (2002) Publisher: American Chemical Society.
7. X Jiaqiang, C Yuping, L Yadong, S Jianian, Gas sensing properties of ZnO nanorods prepared by hydrothermal method. *J. Mater. Sci.* **40**, 2919–2921 (2005).
8. Y Gong, M Zhou, L Andrews, Spectroscopic and Theoretical Studies of Transition Metal Oxides and Dioxygen Complexes. *Chem. Rev.* **109**, 6765–6808 (2009) Publisher: American Chemical Society.
9. HJ Zhai, LM Wang, SD Li, LS Wang, Vibrationally Resolved Photoelectron Spectroscopy of BO- and BO2-: A Joint Experimental and Theoretical Study. *The J. Phys. Chem. A* **111**, 1030–1035 (2007) Publisher: American Chemical Society.
10. AK Patra, A Dutta, A Bhaumik, Self-assembled ultra small ZnO nanocrystals for dye-sensitized solar cell application. *J. Solid State Chem.* **215**, 135–142 (2014).
11. C Clementi, et al., Photoluminescence properties of zinc oxide in paints: a study of the effect of self-absorption and passivation. *Appl. Spectrosc.* **66**, 1233–1241 (2012).
12. SH Jin, et al., Water-Soluble Thin Film Transistors and Circuits Based on Amorphous Indium–Gallium–Zinc Oxide. *ACS Appl. Mater. & Interfaces* **7**, 8268–8274 (2015) Publisher: American Chemical Society.
13. ZL Wang, Zinc oxide nanostructures: growth, properties and applications. *J. Physics: Condens. Matter* **16**, R829–R858 (2004) Publisher: IOP Publishing.
14. A Sirelkhatim, et al., Review on Zinc Oxide Nanoparticles: Antibacterial Activity and Toxicity Mechanism. *Nano-Micro Lett.* **7**, 219–242 (2015).
15. SB Woodley, AA Sokol, CRA Catlow, AA Al-Sunaidi, SM Woodley, Structural and Optical Properties of Mg and Cd Doped ZnO Nanoclusters. *The J. Phys. Chem. C* **117**, 27127–27145 (2013).
16. MJS Spencer, Gas sensing applications of 1D-nanostructured zinc oxide: Insights from density functional theory calculations. *Prog. Mater. Sci.* **57**, 437–486 (2012).
17. J Xu, et al., Uniform ZnO nanorods can be used to improve the response of ZnO gas sensor. *Mater. Sci. Eng. B* **150**, 55–60 (2008).
18. SR Kelly, et al., ZnO As an Active and Selective Catalyst for Electrochemical Water Oxidation to Hydrogen Peroxide. *ACS Catal.* **9**, 4593–4599 (2019) Publisher: American Chemical Society.
19. MA Johar, RA Afzal, AA Alazba, U Manzoor, Photocatalysis and Bandgap Engineering Using ZnO Nanocomposites. *Adv. Mater. Sci. Eng.* **2015**, e934587 (2015) Publisher: Hindawi.
20. E Berardo, et al., Benchmarking the fundamental electronic properties of small tio 2 nanoclusters by gw and coupled cluster theory calculations. *J. Chem. Theory Comput.* **13**, 3814–28 (2017).
21. X Chen, Z Wu, D Liu, Z Gao, Preparation of ZnO Photocatalyst for the Efficient and Rapid Photocatalytic Degradation of Azo Dyes. *Nanoscale Res. Lett.* **12**, 143 (2017).
22. MM Brewster, X Zhou, MY Lu, S Gradečak, The interplay of structural and optical properties in individual ZnO nanostructures. *Nanoscale* **4**, 1455–1462 (2012) Publisher: The Royal Society of Chemistry.
23. G Malloci, L Chiodo, A Rubio, A Mattoni, Structural and Optoelectronic Properties of Unsaturated ZnO and ZnS Nanoclusters. *The J. Phys. Chem. C* **116**, 8741–8746 (2012) Publisher: American Chemical Society.
24. V Srikant, DR Clarke, On the optical band gap of zinc oxide. *J. Appl. Phys.* **83**, 5447–5451 (1998) Publisher: American Institute of Physics.
25. SH Na, CH Park, First-Principles Study of the Surface of Wurtzite ZnO and ZnS - Implications for Nanostructure Formation. *J. Korean Phys. Soc.* **54**, 867–872 (2009) Publisher: The Korean Physical Society.
26. L Wang, M Muhammed, Synthesis of zinc oxide nanoparticles with controlled morphology. *J. Mater. Chem.* **9**, 2871–2878 (1999) Publisher: The Royal Society of Chemistry.
27. R Bovhyra, D Popovych, O Bovgyra, A Serednytski, Ab Initio Study of Structural and Electronic Properties of (ZnO) n "Magical" Nanoclusters n = (34, 60). *Nanoscale Res. Lett.* **12**, 76 (2017).
28. AA Al-Sunaidi, AA Sokol, CRA Catlow, SM Woodley, Structures of Zinc Oxide Nanoclusters: As Found by Revolutionary Algorithm Techniques. *The J. Phys. Chem. C* **112**, 18860–18875 (2008) Publisher: American Chemical Society.
29. CE Szakacs, EF Merschrod S., KM Poduska, Structural Features That Stabilize ZnO Clusters: An Electronic Structure Approach. *Computation* **1**, 16–26 (2013).
30. M Chen, TP Straatsma, Z Fang, DA Dixon, Structural and Electronic Property Study of (ZnO)n, n 168: Transition from Zinc Oxide Molecular Clusters to Ultrasmall Nanoparticles. *The J. Phys. Chem. C* **120**, 20400–20418 (2016) Publisher: American Chemical Society.
31. KDD Gunaratne, C Berkdemir, CL Harmon, AW Castleman, Investigating the Relative Stabilities and Electronic Properties of Small Zinc Oxide Clusters. *The J. Phys. Chem. A* **116**, 12429–12437 (2012) Publisher: American Chemical Society.
32. MJ Frisch, et al., Gaussian~16 Revision C.01 (2016) Gaussian Inc. Wallingford CT.
33. R Dennington, TA Keith, JM Millam, Gaussview Version 6 (2019) Semichem Inc. Shawnee Mission KS.
34. J Matxain, A Irigoras Balda, J Fowler, J Ugalde, Electronic excitation energies of Zn i S i clusters. *Phys. Rev. A* **64**, 013201 (2001).
35. CA Fancher, HL de Clercq, OC Thomas, DW Robinson, KH Bowen, Zinc oxide and its anion: A negative ion photoelectron spectroscopic study. *The J. Chem. Phys.* **109**, 8426–8429 (1998).
36. JH Kim, et al., Vibrationally Resolved Photoelectron Spectroscopy of MgO- and ZnO- and the Low-Lying Electronic States of MgO, MgO-, and ZnO. *The J. Phys. Chem. A* **105**, 5709–5718 (2001) Publisher: American Chemical Society.
37. L Christophorou, *Atomic and molecular radiation physics*, Wiley monographs in chemical physics. No. 0471156299, (year?).
38. Z Fang, DA Dixon, Computational Study of H2 and O2 Production from Water Splitting by Small (MO2)n Clusters (M = Ti, Zr, Hf). *The J. Phys. Chem. A* **117**, 3539–3555 (2013) Publisher: American Chemical Society.